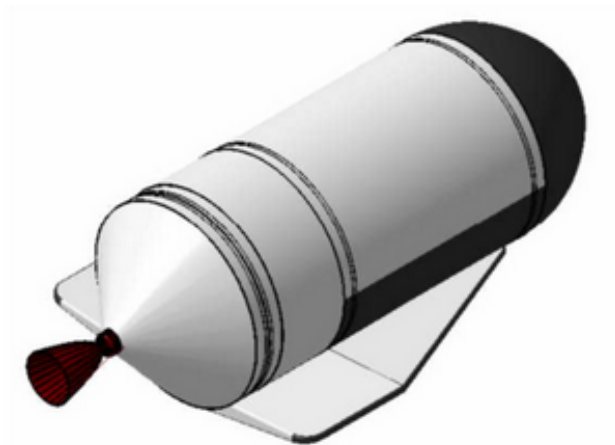

GREDER

Green RE-usable DEbris Remover



Authors :

Tim **Lewis**

Alina **Trifunovic**

Lukas **Krause**

Alexis **Rolin**

Julien **Huynh**

Supervising professor :

Prof. Dr.-Ing. Uwe *Apel*

Version 0.8
February 23, 2020

Contents

1	Schedule	2
1.1	Initial Schedule	2
1.2	Final schedule – comparison as planned and as achieved	3
2	Requirements	5
3	Launcher requirements and launch enveloppe	7
4	Mission analysis	8
5	Satellite catching process	9
5.1	Choice of the process	9
5.2	Magnetic solution	10
5.2.1	Assumptions	10
5.3	Sketching and Calculations	10
6	Heat shield	14
7	Propellant selection	15
7.1	Options overview	16
7.2	Detailed comparison between MON/MMH and H2O2/RP-1	17
7.3	H2O2/RP-1 feasibility check	20
7.4	Summary	21
8	Vehicle design	22
9	Flow schematic	23
10	Mass model	24
10.1	Mass Budget - First Iteration	24
10.1.1	Coefficients & Masses after steps	24
10.1.2	Global equation between m_{UP} and $m_{initial}$	24
10.1.3	First iteration of mass budget	25

10.2	Mass Budget - Second iteration	28
10.2.1	Coefficients & Masses after steps	28
10.2.2	Global equation between m_{UP} and $m_{initial}$	28
10.2.3	Second iteration of mass budget	29
10.3	Frozen information	31
10.3.1	Frozen points	31
10.4	Mass Budget - Final iteration	32
10.4.1	Coefficients & Masses after steps	32
10.4.2	Global equation between m_{UP} and $m_{initial}$	32
10.4.3	Detailed contributors	33
10.4.4	Final mass budget	34
11	Propulsion system	35
11.1	RCS / ACS	35
11.2	Propellant tanks	35
11.3	Pressurization system	35
11.4	Catalyzer	35
11.5	Injectors	37
11.6	Feeding system	37
11.6.1	Line diameters	40
11.6.2	Fuel feeding system	40
11.6.3	Oxidizer feeding system	41
11.7	Turbo pumps	42
11.8	Pressure evolution summary	43
11.8.1	Fuel side	43
11.8.2	Oxidizer side	44
11.9	Engine	44
11.10	Nozzle	44
12	Simulation	45
12.1	Subsystem simulation	45
12.2	System simulation	45
12.3	Simulation preparation and execution	45
12.4	Simulation review	45
13	Lessons learnt	46

Introduction

Ever since the launch of Sputnik 1, the first artificial satellite in October 1957, the number of satellites launched has sharply risen and as of 2020, thousands of satellites are orbiting around the Earth. However, each of every one of those spacecrafts will eventually see their mission being stopped, usually due to a lack of resources from the satellite itself as it reaches the end of its life.

Those who are at the end of their lives will turn into a simple uncontrolled object that keeps orbiting around the Earth and should be avoided as another functioning satellite could take their slot as some of the most important orbits around our planet are starting to get overcrowded and the demand keeps rising.

Moreover, such uncontrolled objects in space can become dangerous as collisions could potentially happen and at such high velocity, those can heavily damage other spacecrafts and create even more debris.

As public awareness grows towards the space debris problem, our mission, Green Debris Remover (GREDER), is looking to contribute to a solution to this problem in a particular orbit, the geo stationary orbit, which is particularly overcrowded due to the many different kinds of satellite operating there.

Chapter 1

Schedule

At the start of the project a dedicated group meeting was performed in order to agree on a common project sequence, tasks and challenges as well as work distribution. This group meeting was deemed essential to structure the work packages and to achieve a consolidated baseline for the whole project including time line.

The result is a complex MS project Gantt diagram, which can be found in Annex 1.

1.1 Initial Schedule

The first version of the schedule starts with a project Kick-Off in October which is afterwards followed by a short planning phase. In this planning phase issues as scheduling, work distribution and scope of the project were addressed.

Subsequently, the definition phase started. Within this phase, the vehicle requirements were defined and the mission was planned, calculated and visualized in MATLAB. The outcomes of the definition phase are the boundary requirements which are set to provide a frame for both: the vehicle itself as well as the propulsion system. The requirements were defined at the beginning of the project and were verified after project completion.

Upon definition of the boundary requirements, the specification phase started. Within this phase, different propellant combinations were identified, discussed and compared. Additionally a first mass budget was calculated. The result of this phase is the system specification.

The sequence of the project includes several presentations. The first one was performed in October for a quick overview on the project planning. The second one after the boundary requirements and system specification was set. After this presentation, the vehicle and

sub system design phase started. This phase included major parts of the work packages including propulsion system design with all sub-assemblies as RACS/ACS, propellant tanks, feeding and pressurization system, turbo pumps, catalyzer, engine, injector and nozzle. The outcome of this phase is a preliminary vehicle design and sub system design which was presented in the mid-term presentation.

As a last major work package the simulation phase started. The whole system was simulated including all sub systems and additionally the complex H₂O₂ decomposition regulation. The final presentation was performed after all tasks were completed and the simulation was finalized.

An overview the compressed initial schedule is shown in Figure 1.1. The detailed Gantt schedule can be found in Annex 1.

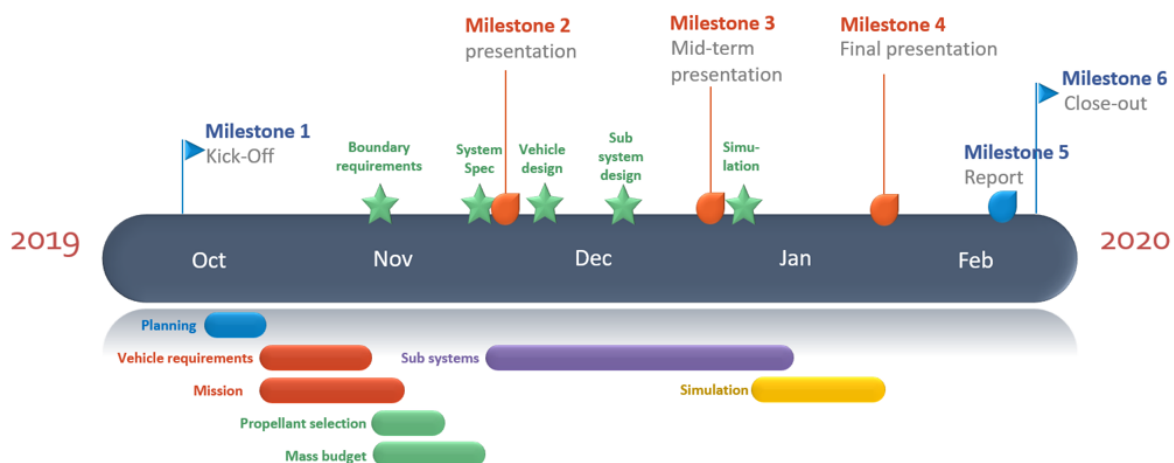


Figure 1.1: Initial schedule

1.2 Final schedule – comparison as planned and as achieved

As usual in project management and project work, not all milestones were achieved in time. As it is shown in the compressed final schedule in Figure 1.2, the finalized vehicle design, the finalized sub system design and the corresponding simulation shifted within the project schedule (Figure 1.2, shown in red). Nevertheless all work packages have been successfully completed until Milestone 4, the final presentation.

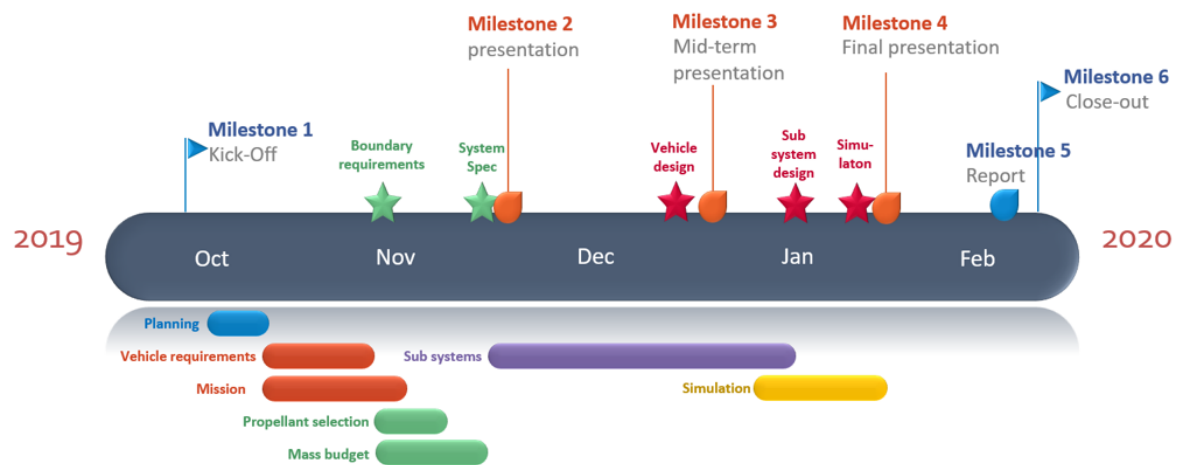


Figure 1.2: Final schedule - comparison as planned and as achieved

Chapter 2

Requirements

The top level requirements for the vehicle and propulsion system are divided in three categories: operation, environment and vehicle. The operation requirements are related to the propulsion system and its applicability for the planned missions. The environmental requirements are defined to ensure that both the vehicle and propulsion system is capable of operating and sustaining during launch, mission and in space environment. The scope of the vehicle requirements is to cover the major parts of the planned mission as refuel-ability, aero braking or accuracy.

Operation	
TL-1	Provide sufficient thrust for completion of the mission profile including a safety margin
TL-2	Re-ignitable at least 1000 times
TL-3	Service life time of at least 100 missions or 25 years in orbit
TL-4	Ignition and functional reliability shall be higher than 99,5%
Environment	
TL-5	Withstand the launch phase
TL-6	Operate in vacuum
TL-7	Operate in an ambient temperature range of 1K to 5K
TL-8	Withstand the temperature gradients resulting from areas turned towards or away
TL-9	Sustain space-related radiation throughout it's complete life time
TL-10	Withstand debris impact of under 1cm diameter with a max relative speed of 15 km/s
Vehicle	
TL-11	The engine shall be the main propulsion system of a GEO satellite recovery vehicle
TL-12	Refuelable between missions
TL-13	Perform aerobrake maneuvers in Earth's atmosphere.
TL-14	Control flight path in Earth's atmosphere using non-propulsive flight control systems
TL-15	Remain within the ARIANE 6/Falcon 9 payload launch capabilities to LEO.
TL-16	Remain on it's guided trajectory with less than 0.1% deviation.

Table 2.1: Requirements for the vehicle

Chapter 3

Launcher requirements and launch enveloppe

Chapter 4

Mission analysis

Chapter 5

Satellite catching process

5.1 Choice of the process

In order to catch and de-orbit a satellite in GEO, we considered the following usable tools :

- Net
- Harpoon
- Claw
- Magnet

Other solutions such as towing the satellite or simply removing them from GEO were not considered as they either did not fit our program or would create too much strain on our spacecraft.

We then took a closer look at the feasibility of each solution and compared the advantages and disadvantages :

Solution	Advantages	Drawbacks	Feasibility
Net	Cheap, simple, low mass	Slow, hard to handle	Yes (JAXA, ESA)
Harpoon	Fairly cheap	Can create more debris	Yes (ESA)
Claw	Safer	Mechanical, moving parts	WIP (CleanSpace One)
Magnet	Adjustable, no moving parts	Higher mass, needs power	Research State

As the main focus of our mission is reliability and re-usability, we made the choice of using magnets to catch and hold the satellite we would like to de-orbit.

5.2 Magnetic solution

Even though we decided that we would use magnets, we needed to make sure it was feasible and to lower the drawbacks related to this solution as much as possible. The first precision we need to make is that we will be using electromagnets in order to regulate the intensity of the current in the coil of it, thus, modulating the attraction force so the contact between our spacecraft and the satellite will not be made at high velocity, avoiding damages and space debris creation.

Even though it is still at the state of research, we believe that using electromagnets as our catching solution is realistic as both ESA (with ISAE SupAero) and the NASA have been considering and studying this solution since 2017.

However, as a matter of complexity, we will have to make assumptions in order to simplify the problem. The objective in this part is to prove that, with assumptions, this solution can be applied to our mission and to find the required energy to both catch and hold the satellite until its release.

5.2.1 Assumptions

In our calculations, we assumed that :

1. We can consider the magnetic circuit between GREDER and the nozzle of the satellite is a closed one (no air gaps)
2. About 0.1% of the satellite's mass is magnetically operable
3. Mutual attraction is relatively low compared to the magnetic force
4. Residuals in the alloy of the magnets' cores are neglectable

5.3 Sketching and Calculations

Using the first assumption, we can use the formula for the magnetic force in a magnetic circuit with no air gap :

$$F = \frac{(\mu NI)^2 A}{2\mu_0 L^2} \quad (5.1)$$

With :

- μ the magnetic permeability of the core of our magnet (determined by the alloy)
- N the number of turns of the coil around the core

- I the current running through the coil
- A the cross section area of the core
- μ_0 the magnetic constant
- L the length of the mean magnetic circuit

In order to have a good balance between thermal properties and magnetic properties we decided to use an alloy made of 90% of iron and 10% of cobalt for our core. We decided to use this alloy as iron has the best magnetic properties (high relative magnetic permeability) and added cobalt as it has a higher Curie Temperature than iron but has a lower relative magnetic permeability.

In terms of magnet design, we chose to use a squared cross section of $5\text{cm} \times 5\text{cm}$ for the magnet core and with a length of 15cm , made of an iron-cobalt alloy and a copper coil around it. We decided to have 135 turns of the coil around the core with a coil diameter of 1mm in order to not have the wire revolutions stuck to each other. We also want to run a current of 10A through the coil.

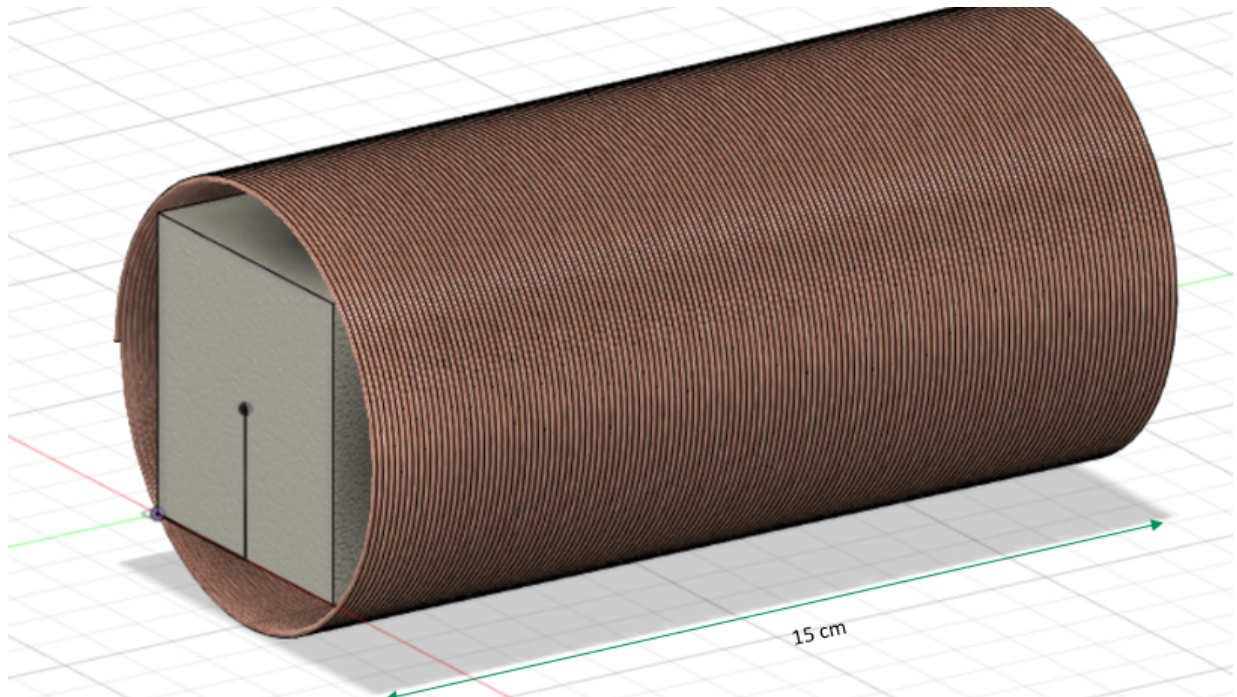


Figure 5.1: CAD of a catching magnet

With those design choices we get the following parameters while taking into consideration that there should not be any kind of residuals in the core alloy :

- $\mu_0 = 4\pi \times 10^{-7} \text{ H/m}$
- $\mu = \left(\frac{\mu_{iron} + \mu_{cobalt}}{2} \right) \times \mu_0 = 5.868 \times 10^{-3} \text{ H/m}$
- $N = 135 \text{ turns}$
- $I = 10 \text{ A}$
- $A = 25 \text{ cm}^2 = 2.5 \times 10^{-3} \text{ m}^2$
- $\rho_{core} = \rho_{iron} \times 0.9 + \rho_{cobalt} \times 0.1 = 7.9726 \text{ g/cm}^3$
- $\rho_{coil} = \rho_{copper} = 8.96 \text{ g/cm}^3$

We then need to find the length L of the mean magnetic circuit. In order to do so, we decided to start the catching sequence at 10 *m* from the satellite and that the target has an exploitable nozzle of 40 *cm* of diameters which is realistic for spacecrafts in the mass range of 3 500 *kg*. We could then sketch the catching sequence as so (not to scale) :

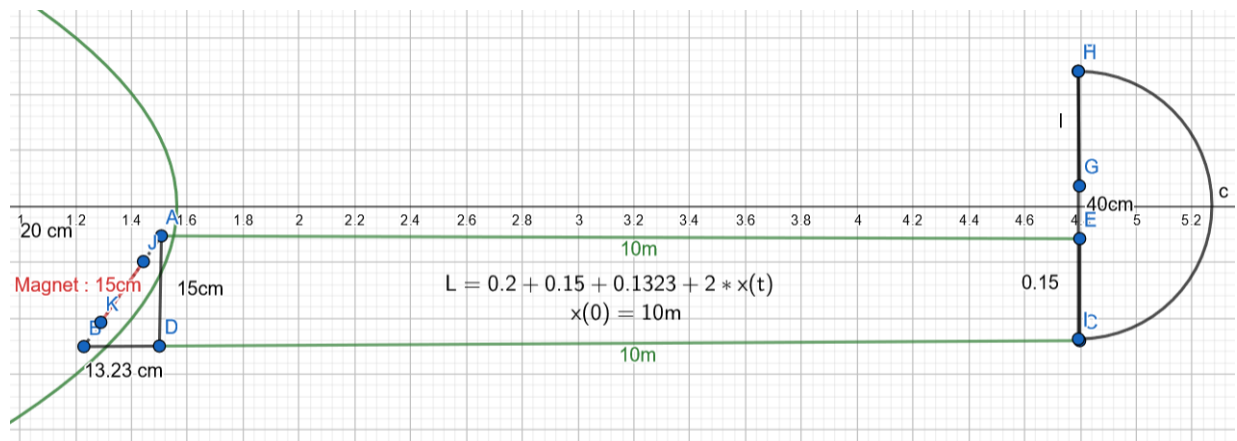


Figure 5.2: Catching sequence (not to scale)

We can then have the length L as a function of the distance between the tip of our spacecraft and the nozzle of our target. As a result we can proceed to find the feasibility of our solution with this magnet design by finding the time it would require at this state to attract the target. However, in this case, the current modulation when the target is close has not been modeled due to its complexity.

Considering that the force will be on one axis only and $m = 0.001 \times m_{target} = 3.5 \text{ kg}$:

$$\vec{F} = m\vec{a} \quad (5.2)$$

$$\frac{(\mu NI)^2 A}{2\mu_0 L(x)^2} = m \times \ddot{x} \quad (5.3)$$

$$\frac{(\mu NI)^2 A}{2\mu_0 [0.2 + 0.15 + 0.1323 + 2x(t)]^2} = m\ddot{x}(t) \quad (5.4)$$

$$\frac{(\mu NI)^2 A}{2\mu_0 [0.4823 + 2x(t)]^2} = m\ddot{x}(t) \quad (5.5)$$

The catching time can then be found using *ode45* on Matlab :

```

1 clearvars; clc;
2 catchtime = 1;
3 x0 = 10;
4 while 1
5     [t,x] = ode45(@f3,[0:1:catchtime], [x0; 0; 0; 0]);
6     if (x(catchtime ,1) >= 2 * x0)
7         break
8     else
9         catchtime = catchtime +1;
10    end
11 end

```

And the function used for the *ode* solver :

```

1 function [Xdot] = f3(t, X)
2 mu = 5.686e-3; mu0 = 4 * pi * 10 ^(-7);
3 N = 135; I = 10; A = 0.05 ^ 2; m = 3500 ;
4 x = X(1); y = X(2); vx = X(3); vy = X(4);
5 Fmag = (mu * N * I) ^2 * A / (2 * mu0 *(2 * norm(X(1:2)) + 0.4823) ^ 2 );
6 Xdot = [vx; vy; 0.001 * Fmag / m; 0];
7 end

```

We then get a catching time of 812 seconds. As a result, we can determine the energy required to operate the magnets aswell as their masses and volumes. We are considering a holding time for approximately half an hour and we also need to verify that the magnets will be able to hold the target while we are de-orbiting.

Chapter 6

Heat shield

Chapter 7

Propellant selection

For the propellant selection for our vehicle, several important aspects have to be taken into account including:

- Specific impulse in vacuum (Isp) of the propellant
- Storability
- Toxicity including ground handling
- Costs (while the main cost driver is not the propellant itself more its toxicity)
- Reasonable refueling options due to the desired mission profile of the vehicle
- Space flight heritage of the propellant (e.g. flight proven, ground proven or in development)
- Density specific impulse
- Corrosive behavior and compatibility with typical light weight tank materials as titanium or aluminum
- and many more

At first several possible and typical flight proven propellant combinations were analyzed and the most promising combinations were selected and then compared in detail. Afterwards a feasibility study for the chosen propellant combination was deemed necessary in order to check whether the desired propellant combination is able to perform the required mission and de-risk the next development steps.

7.1 Options overview

In literature and historical research several reasonable and flight proven propellant combinations have been found. The propellant combinations are divided in three sub-categories: petroleum, cryogenics and hypergolic. These combinations are all bipropellant combinations, the monopropellants have already been excluded at the beginning due considerably low specific impulse in comparison to bipropellants and therefore not suitable for the intended mission profile.

Petroleum fuels are containing a combination of complex hydrocarbons and have been refined from mineral oil. The typical petroleum used as rocket fuel is a highly refined kerosene, called RP-1 (rocket propellant 1). In bipropellant use an oxidizer is necessary and therefore petroleum is often mixed with LOX (liquid oxygen). The specific impulse of a petroleum fuel and cryogenic oxidizer combination is higher than for hypergolic propellant combinations but lower than for fully cryogenic options.

The cryogenics are gaseous bipropellants stored at very low temperatures and usually stand out due to their high specific impulse. The most common cryogenics are liquid hydrogen and liquid oxygen which have to be stored at -253°C for LH2 and -183°C for LOX. Recently, cryogenic combinations with liquid methane (LCH4) as fuel are receiving more attention due to availability methane on mars and therefore it might become attractive for future mars missions.

The last group in this option overview are the hypergolics. The hypergolics are bipropellants that ignite spontaneously when in contact. The main advantage of hypergolics is the storability. Hypergolics are liquid at room temperature and therefore no additional heating or cooling is necessary during the mission. Nevertheless the hypergolics provide less specific impulses than cryogenics and they are mostly highly toxic.

Table 7.1 shows a comparison of different bipropellants divided in the three above mentioned categories. In the initial comparison of this chapters the propellant combinations are compared with regards to their major characteristics: specific impulse, flight evidence and therefore technical risk, storability and their reasonability for our application.

It is clearly visible that most propellant combinations have not been found reasonable for our application due to low temperature storage. Our vehicle is designed to perform several missions with several ignitions permission and refueling at an in orbit refueling station – this mission profile is not conformable with constant low temperature storage.

In contrast to that the group of hypergolics offers great storability and good specific impulse for the mission profile and a storage of these propellants at an in orbit refueling

7.2. Detailed comparison between MON/MMH and H2O2/RP-1 Page 17/55

station is feasible. Since the two options MON/MMH and H2O2/RP-1 are promising, further in depth analysis was deemed necessary.

Type	Combination	Isp [s] vacuum	Flight proven	Storability	Toxicity	Reason- able for our applicati on
Petroleum	LOX / RP-1	300-353	Used for the lower stages of the Soyuz boosters, and the first stage of the U.S. Saturn V, Atlas, and Falcon 9 boosters. Very similar to Robert Goddard's first rocket.	LOX low temperature storage	non-toxic	NO
Cryogenic	LOX / LH2	420-453	Used in the stages of the Space Shuttle, Space Launch System, Ariane 5, Delta IV, New Shepard, H-IIB, GSLV and Centaur.	low temperature storage	non-toxic	NO
	LOX / LCH4 (methane)	355	NO	low temperature storage	non-toxic	NO
	LF2 (flourine) / LH2	470	NO	low temperature storage	highly toxic	NO
Hypergolic	MON / MMH	321-336	three first stages Proton booster, Indian Vikas engine for PSLV and GSLV rockets, most Chinese boosters, a number of military, orbital and deep space rockets	storable	highly toxic	YES
	H2O2 / RP-1	313	British gamma rocket engines (65kN 2nd stage for example)	storable	non-toxic	YES

Table 7.1: Propellant combinations overview

7.2 Detailed comparison between MON/MMH and H2O2/RP-1

The hypergolic propellant combination MON/MMH and H2O2/RP-1 have been found reasonable for our mission and application. Table 7.2 shows a detailed comparison of the propellant combinations. Several characteristics were found to be minor and others were found to be major for our application. The major characteristics are the vacuum specific impulse, the tank volume ration, the combined density, the density specific impulse and the toxicity and storability (highlighted in yellow).

Both propellant combinations have a comparable specific impulse. Therefore no favor

for either MON/MMH or H₂O₂/RP-1.

The tank volume ratio is better for MON/MMH because the ratio is nearly one to one, therefore both oxidizer and fuel tank could share the same tank design. This would significantly decrease the development costs since no second tank design and second qualification tank is necessary. Also the manufacturing costs would decrease due to more possibilities of batch production. Especially production costs of forged tank hemispheres are a huge cost driver and these would decrease due to non-recurring costs being distributed on a larger number of hemispheres. Also the costs for jigs and tools would decrease. This favors MON/MMH.

The combined density for H₂O₂/RP-1 is slightly better than for MON/MMH. Nevertheless the combined density is not a significant value without taking the specific impulse into account. Calculating the density specific impulse, which is basically the specific impulse per mass, H₂O₂/RP-1 exceeds MON/MMH by 12%. In this category H₂O₂/RP-1 is the winner because it can provide more specific impulse per mass.

Comparing toxicity of MON/MMH to H₂O₂/RP-1 it can be stated that MON/MMH is highly toxic and has to be handled with extreme care which increases the ground handling costs of this propellant combination. In contrast to that is the toxicity of H₂O₂/RP-1. This propellant combination is non-toxic and can be considered as “green” propellant. Nevertheless careful ground-handling is also necessary for this combination because it is prone to reaction with trace elements. H₂O₂/RP-1 succeeds in this category.

The last category is the storability. Since both propellant combinations are storable in liquid/liquid condition both propellants are suitable for the application.

Taking all criteria and results into account H₂O₂/RP-1 is the preferred propellant combination for our application. The main reasons are:

- comparable specific impulse to MON/MMH
- better density specific impulse
- non-toxic advantage for maintenance at refuel station
- good on-ground handling
- possibility of R&D funds by ESA for green debris remover

The main reason against MON/MMH is the toxicity.

	MON / MMH	H2O2 / RP-1
Isp vacuum [s]	321-336	335
state at 20 °C	liquid / liquid	liquid / liquid
phase transus solid/gaseous	[-52 °C; 87 °C] / [-11 °C; 21 °C]	[-0,4 °C; 142 °C] / [-60 °C; 300 °C]
Densities [kg/m ³]	1450 / 900	1440 / 900
Viscosity [mPa·s]	0,86 / 0,48	1,19 / 0,8
Vapor pressure at 20 °C [bar]	0,05 / 1,1	0,003 / 7,5
Mixture ratio [Parts of Oxidator]	1,6	7
Tank volumes per 1000kg propellant [l]	424,4 / 427,4 total 851,6	607,6 / 138,9 total 746,5
Tank volume ratio	1 to 1,007	1 to 0,23
Combined density [kg/m ³]	1240	1370
Density specific impulse [Kg*s/m ³]	409200	458950
Chamber temperature [K]	3330	2900
Toxicity	highly toxic	non -toxic
Storability	storable	storable
Corrosion	highly corrosive	slightly corrosive
Compatible materials	for example Titanium, Aluminum	High purity aluminum (Al95), stainless steel (304, 304L, 316, 316L)
Isp mono propellant mode [s]	250 / N/A	160 / N/A
Flight proven	3 first stages Proton booster, Indian Vikas engine for PSLV and GSLV rockets, most Chinese boosters, a number of military, orbital and deep space rockets	British gamma rocket engines (65kN 2nd stage for example)

Table 7.2: Detailed propellant comparison MON/MMH and H2O2/RP-1

Propellants	Engine name	Engine type	Engine status	Fvac (kN) Vacuum thrust	OF Ox to fuel ratio	I svac (N-s/kg) Specific vacuum impulse	[ms/mp] Ratio stage empty mass (ms) over total propellant mass (mp)	Calculated Δv [km/s]
H2O2(~0.97)-RP1	RD161P	Upper stage, unknown	Development	24.5 to 14.7	5,9	3128	[--]	[--]
H2O2(~0.83)-RP1	Gamma-2	Upper stage, Pump fed	Flown	68.2	8,23	2599	0.18	4,46
H2O2(--)-RP1	BA-44	Upper stage, Pressure fed	Development	196 to 98	7,5	2941	0.08	7,43
H2O2(--)-RP1	BA-810	Upper stage, Pressure fed	Development	3600 to 1800	7,5	2765	0.08	6,98
								required $\Delta v=6,61$

Table 7.3: Historical data of flight H2O2/RP-1 engines

7.3 H2O2/RP-1 feasibility check

Since H2O2/RP-1 is not a common propellant combination and not as frequently used space industry as MON/MHH a further feasibility study has to be performed:

- to de-risk the next development steps
- to check whether the desired propellant combination is able to perform the required mission

In 7.3 historical data of flight H2O2/RP-1 engines is analyzed. One of the engines “Gamma-2” was flown, the others were in development. The thrusts of all engines are comparable or higher than foreseen for our application and two engines also operate in comparable delta-v ranges. This leads to the conclusion that a H2O2/RP-1 engine is generally speaking feasible.

7.4 Summary

In summary H₂O₂/RP-1 is a viable non-toxic hypergolic propellant combination with a good density specific impulse. Additionally the propellant combination is supported by historical flight data. Therefore all further steps will be based on this combination.

Chapter 8

Vehicle design

Chapter 9

Flow schematic

Chapter 10

Mass model

10.1 Mass Budget - First Iteration

Before actually going into our mass budget, we wanted to get a reference idea for the propellant mass so that we would be sure to be able to achieve our Δv . In order to get this, we decided to find a relation between the usable propellant mass and the mass of the rest as a ratio. This is then fixed and will also allow us to know roughly how much propellant we need depending on the dry mass. Let m_{UP} be the mass of usable propellant. Moreover, we would be aiming for a total initial mass of roughly 20 to 25t on our last iteration. This first iteration was done with another magnet design, presented in November which consisted in two large discs of 600 kg each and have then been abandoned for the second iteration.

10.1.1 Coefficients & Masses after steps

Considering that $ISP = 295s$ and annotating $\frac{m_{UP_i}}{m_{total_i}} = K_i$ with i the burn number :

Step	Required Δv in m/s	K_i	Mass after step
1	2802.4	0.620	$0.38 m_{initial}$
2	1342.2	0.371	$0.239m_{initial}$
3	522.9	0.165	$0.200m_{initial}$
Satellite caught	NA	NA	$0.2m_{initial} + 3500$
4	1487.8	0.402	$0.1196m_{initial} + 2093$
Satellite release	NA	NA	$0.1196m_{initial} - 1407$
5	5.3	0.002	$0.1194m_{initial} - 1404.186$
6	72.4	0.0247	

10.1.2 Global equation between m_{UP} and $m_{initial}$

Step	$\frac{m_{UP}}{m_{initial}}$	Bias due to debris
1	0.620	0
2	0.141	0
3	0.039	0
4	0.0804	1407
5	0.00024	-2.814
6	0.00295	-36.68
TOTAL	0.88359	+1369.506

We then get our general relation between the usable propellant mass and the initial mass

$$m_{prop} = 0.88359m_{init} + 1369.506$$

And as $m_{initial} = m_{UP} + m_{rest}$:

$$m_{prop} = \frac{1}{0.11641} \left[0.88359m_{rest} + 1369.506 \right]$$

m_{rest} includes the dry mass and the propellant required for the ACS.

10.1.3 First iteration of mass budget

Sub systems

Contributor	Mass in kg
<u>EPS</u>	-
Fuel cells	165.6727
H2 for fuel cell (tank included)	10
Cables	20
GNC	5
Batteries	61.3333
Actuators (for flaps)	10
Servos	1
<u>On board computer</u>	5
<u>Telecommunications</u>	10
<u>Thermal control</u>	10
<u>ACS/RCS</u>	-
Reaction wheels	106
ACS (without propellant)	36.16
<u>Total</u>	440.166

Payload

Contributor	Mass in kg
Magnet	1200

Structure

Contributor	Mass in kg
Hull	509
Wing	54
Engine	60
Engine frame	51
Connectors	25
Tanks	350
Heat shield	472
<i>Total</i>	1521

Others

Contributor	Mass in kg
Catalyzer	10
Lines	25
ACS including Propellant	672
Non usable propellant (Residuals, transient, etc.)	200
Helium (including tank)	30
<i>Total</i>	937

We then get

$$m_{rest} = m_{Subsystems} + m_{Payload} + m_{Structure} + m_{Others} = 4098.166kg$$

Which, with the previously obtained equation :

$$m_{UP} = 42\,870.926kg$$

As the mixture ratio is $MR = 7.07$ and $m_{UP} = m_{UF} + m_{UOP}$

$$m_{UsableFuel} = \frac{m_{UP}}{1 + MR} = 5\,312\,kg$$

$$m_{UsableOxidizer} = MR \times m_{UsableFuel} = 37\,559\,kg$$

Results

We can sum this first iteration up with the following table :

Contributor	Mass (kg)
Structure	1 521
Magnets	1 200
Sub Systems	440.166
Tank Pressurization	30
Engine	60
Catalyzer	10
Lines	25
Dry mass	3 286.166
Non usable propellant	200
ACS/RCS Propellant	142.12
Usable propellant	42 870.926
Total initial mass	46 969.092

This first initial mass is way over what we are targeting and there are many parameters to be refined during the next iteration.

10.2 Mass Budget - Second iteration

After refining multiple parameters and fixing others to get more accurate values, we went into the second iteration of our mass budget. Having our I_{SP} changed also required another iteration in our calculation formula between the usable propellant mass the the rest of the mass.

10.2.1 Coefficients & Masses after steps

Considering that $ISP = 315s$ and annotating $\frac{m_{UP_i}}{m_{total_i}} = K_i$ with i the burn number :

Step	Required Δv in m/s	K_i	Mass after step
1	2802.4	0.596	$0.404 m_{initial}$
2	1342.2	0.352	$0.261792m_{initial}$
3	522.9	0.156	$0.221m_{initial}$
Satellite caught	NA	NA	$0.221m_{initial} + 3500$
4	1487.8	0.382	$0.137m_{initial} + 2163$
Satellite release	NA	NA	$0.137m_{initial} - 1337$
5	5.3	0.0017	$0.1368m_{initial} - 1334.73$
6	72.4	0.023	

10.2.2 Global equation between m_{UP} and $m_{initial}$

Step	$\frac{m_{UP}}{m_{initial}}$	Bias due to debris
1	0.596	0
2	0.142	0
3	0.041	0
4	0.084	1337
5	0.0002	-2.273
6	0.0032	-30.699
TOTAL	0.8664	+1304.028

This time our equation between those two masses is given by

$$m_{UsableProp} = \frac{1}{0.1336} \left[0.8664m_{rest} + 1304.028 \right] \quad (10.1)$$

10.2.3 Second iteration of mass budget

As our way of presenting our first iteration of the mass budget didn't seem clear enough to us, we decided to present it in another, more logical way : **Structure**

Contributor	Mass (kg)
Hull	192
Tanks (including non usable propellant)	700
Wings	136
Lines	60
Connectors	16
H_2 tank	12
Structure	1 116

Electrical related contributors

Contributor	Mass (kg)
Batteries	241
Fuel cells	202
On Board Computer	5
Cables	20
H_2 for fuel cells	5
Wing actuators	10
Telecommunications	10
GNC	5
Thermal Control	10
Magnets (Payload)	25.65
Electrical related contributors	533.65

ACS and RCS

Contributor	Mass (kg)
Thrusters	36
H_2O_2	90
Reaction wheels	106
ACS & RCS	232

Propulsion

Contributor	Mass (kg)
Engine	93
Turbopumps	25
Pressurization (He)	1.3
Catalyzer	30
Propulsion	149.3

With those tables, we can deduce m_{rest} :

$$m_{rest} = m_{Structure} + m_{Elec} + m_{ACS\&RCS} + m_{Propulsion} \quad (10.2)$$

$$m_{rest} = 2\,030.95\,kg \quad (10.3)$$

Thus,

$$m_{UsableProp} = \frac{1}{0.1336} \left[0.8664 m_{rest} + 1304.028 \right] \quad (10.4)$$

$$m_{UsableProp} = 22\,931\,kg \quad (10.5)$$

$$m_{Fuel} = \frac{m_{UsableProp}}{MR + 1} \quad (10.6)$$

$$m_{Fuel} = 2841.6\,kg \quad (10.7)$$

$$m_{Ox} = m_{UsableProp} - m_{Fuel} \quad (10.8)$$

$$m_{Ox} = 20\,089.89\,kg \quad (10.9)$$

$$m_0 = 24\,962.41\,kg \quad (10.10)$$

In this second iteration with a better I_{sp} and refined values for all of the contributors, we have a large improvement as our initial mass decreased drastically.

10.3 Frozen information

After our second iteration of the mass budget, we decided to make a list of the fixed values that we will work around in our further design.

10.3.1 Frozen points

- We will do 20 aerobrakes
- We will have a separate tank design
- H_2O_2 will be pressurized by its decomposition
- The decomposition control will be managed by rotation of the spacecraft
- ACS/RCS Layout similar to the Space Shuttle
- H_2O_2 catalyzers separate
- H_2O_2/O_2 separation via thermodynamic properties
- H_2/O_2 will be used in fuel cells to produce energy

Data	Value	Unit
Empty raw mass	2 031	kg
Usable propellant	22 931	kg
Total mass	24 962	kg
Flowrate	10	kg/s
Rocket diameter	2	m
$I_{spvacuum}$	335	s
Thrust $F = \dot{m}I_{sp}g_0$	32863.5	N
Mixture Ratio	7.07	-
Wall thickness	TBA	m
H_2O_2 internal pressure	1.35	bar

10.4 Mass Budget - Final iteration

As the fixed I_{sp} has been refined as well as other parameters, we went into our final iteration of the mass budget with the same process as the two previous ones.

10.4.1 Coefficients & Masses after steps

Considering that $ISP = 335s$ and annotating $\frac{m_{UP_i}}{m_{total_i}} = K_i$ with i the burn number :

Step	Required Δv in m/s	K_i	Mass after step
1	2802.4	0.574	$0.426 m_{initial}$
2	1342.2	0.335	$0.283 m_{initial}$
3	522.9	0.148	$0.241 m_{initial}$
Satellite caught	NA	NA	$0.221 m_{initial} + 3500$
4	1487.8	0.364	$0.153 m_{initial} + 2226$
Satellite release	NA	NA	$0.153 m_{initial} - 1274$
5	5.3	0.0016	$0.1528 m_{initial} - 1271.96$
6	72.4	0.0218	

10.4.2 Global equation between m_{UP} and $m_{initial}$

Step	$\frac{m_{UP}}{m_{initial}}$	Bias due to debris
1	0.574	0
2	0.143	0
3	0.042	0
4	0.088	1274
5	0.0002	-2.038
6	0.0033	-27.73
TOTAL	0.8505	+1244.232

Thus,

$$m_{UsablePropellant} = \frac{1}{0.1495} [0.8505 m_{rest} + 1244.232]$$

10.4.3 Detailed contributors

Structure

Contributor	Mass (kg)
Hull	192
Tanks	700
Wings	136
Lines	70
Connectors	16
Brackets	35
H_2 Tanks	12
Structure	1161

Electrical systems

Contributor	Mass (kg)
Batteries	369.03
Fuel cell	202
OBC	10
Cables	57
H_2 for fuel cells	5
Wing actuators	10
Data transmission	20
GNC	10
Thermal control	20
Magnets	25.65
Electrical systems	728.68

Attitude control

Contributor	Mass (kg)
Thrusters	36
H_2O_2 for the ACS	90
Reaction wheels	106
Attitude control	232

Propulsion

Contributor	Mass (kg)
Engine	93
Turbopumps + Electric motors	180
<i>He</i> for pressurization	1.3
Catalyzer	40.86
Propulsion	315.16

10.4.4 Final mass budget

Contributor	Mass (kg)
Structure	1161
Electrical systems	728.68
Attitude control	232
Heat shield	360
Propulsion	315.16
m_{rest}	2796.84
m_{UP} with a 5% performance window	25 508
m_{Fuel}	3160
m_{Ox}	22 347
Initial wet mass	28 304

Chapter 11

Propulsion system

11.1 RCS / ACS

11.2 Propellant tanks

11.3 Pressurization system

11.4 Catalyzer

Besides the advantages of H_2O_2 there is one major drawback that we have take into account. This drawback is that H_2O_2 needs to be decomposed in O_2 and H_2O in order to react with RP-1.

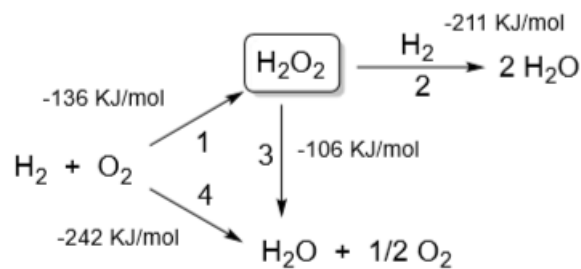


Figure 11.1: H_2O_2 chemical decomposition process

This decomposition is natural but at a low rate whereas we need a very high decomposition rate in order to feed the combustion chamber and sustain a proper flame. This decomposition is an exothermic decomposition. That's why we need a catalyser.

This catalyser needs to be placed between the turbo pump and the injectors. It allows to decompose the H_2O_2 at the last time.

The way a catalyser works is pretty simple; the H_2O_2 goes through a catalyst bed of silver pellets, reacts and generates heat. Why silver ? We chose silver because is the mostly used catalyser for H_2O_2 . However, a lot of other different material exists, like Platinum, Manganese or even Gold but these materials are rarely used due to their cost and also the fact that they need to be made in complex alloy in order to optimize the reaction.

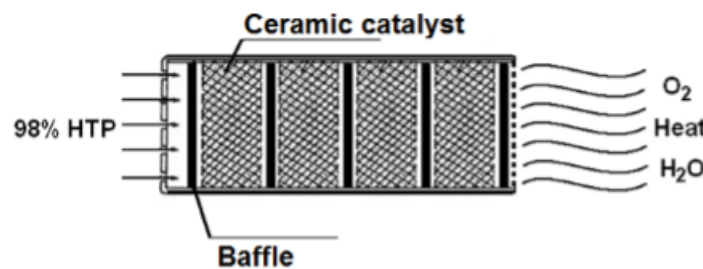


Figure 11.2: Example of catalyst bed

The figure above shows basically how a catalyser works. To have an idea of the shape of ours we just have to swap the ceramic catalyst by silver catalyst. So, it will be a steel cylinder filled with small spherical silver pellet separated by some baffles (silver grid mesh).

An important characteristic of the catalyser is the pressure drop it creates. This pressure drop influences the whole feeding system, the turbo pump sizing and even the injector design. that's why we need to characterize the pressure drop created by the catalyser. In order to do so, we are going to use the Ergun equation for packed bed reactor:

$$\frac{\Delta p}{L} = 151.2 \frac{\mu}{d^2} \frac{(1 - \epsilon)^2}{\epsilon^2} u + 1.8 \frac{\rho}{d} \frac{1 - \epsilon}{\epsilon^3} u^2$$

With μ the dynamic viscosity, ϵ the porosity, d the pellet diameter, ρ the density, L the length of the bed and u the velocity.

In this equation we need some important component such as ϵ . The porosity is complicated to compute and need to be model. According to a recent research we determined a porosity of 0.3802 with a pellet diameter of 5mm.

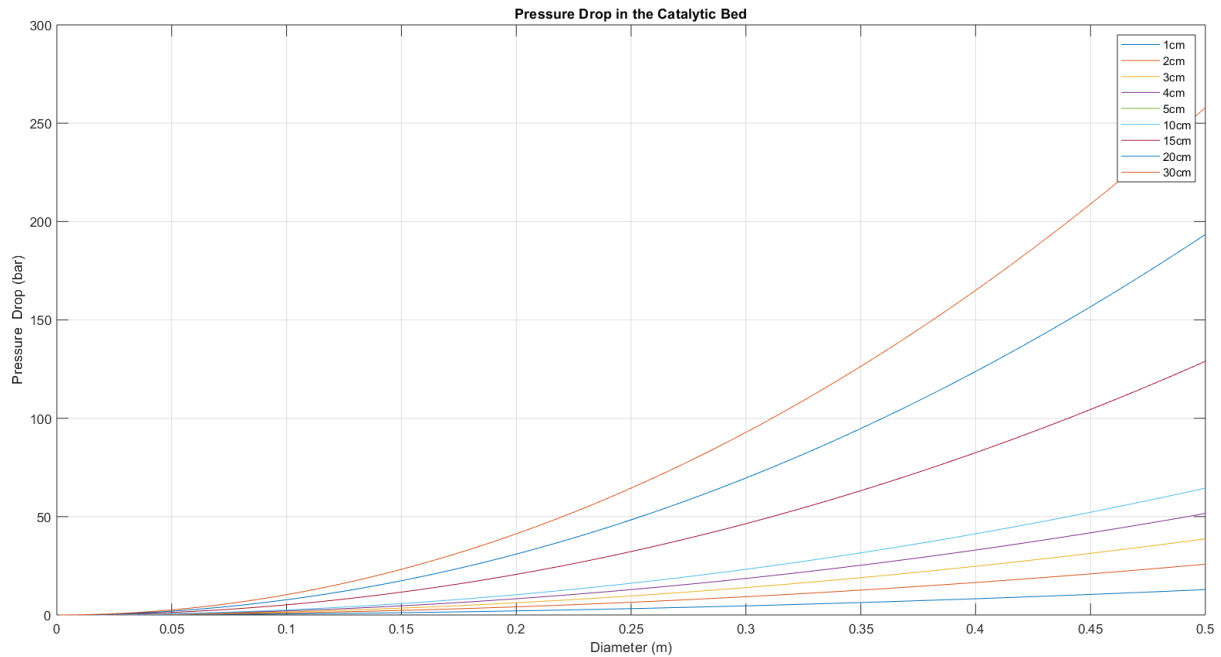


Figure 11.3: Pressure drop depending on the size of the catalyst bed

We see on the graph that the pressure drop rise quickly with the size of the bed. So we need to limit the size of our catalyser in order to not oversize the turbo pump. To do so, we chose to limit our pressure drop to around 30 bars. Finally we obtain a cylinder of 20 cm of diameter and 20 cm of length.

This geometry allows the catalyser to provide a sufficient decomposition rate, a "contained" pressure drop and size. It also generates a great heat as high as $1000K$ at the exit of the catalyst bed.

11.5 Injectors

11.6 Feeding system

After having designed most of our propulsion system. We need to carefully link them by designing our feeding system. The biggest challenge is to create a system that will both fit in our spacecraft and deliver the right amount of propellant from the tanks to the engine through our different, required other subsystems.

The general pressure loss in a system is given by :

$$\Delta P = K \frac{\rho}{2} w^2$$

With K depending on the type of change in system geometry as follow :

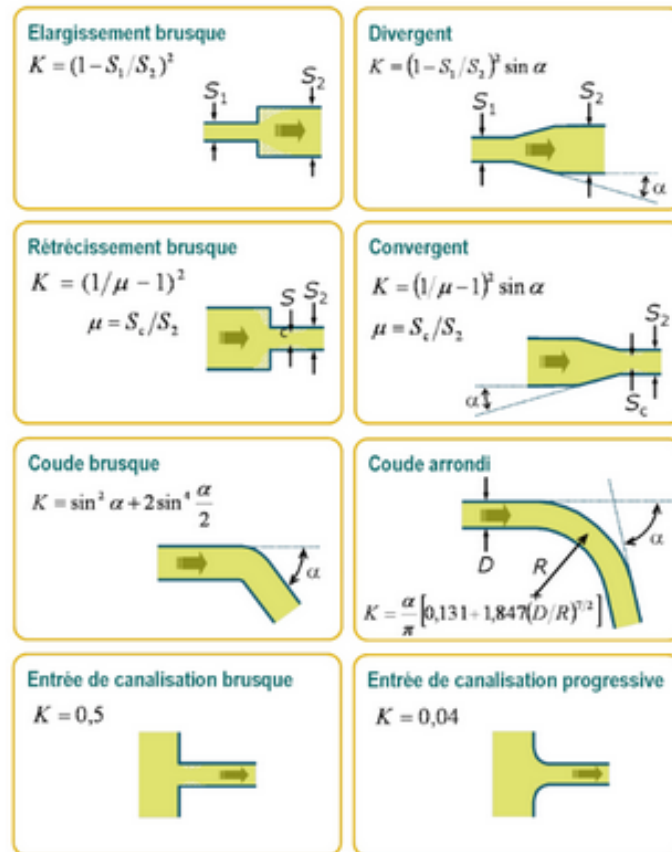


Figure 11.4: K values for geometry changes

In our case, we will use the progressive line entering loss $K = 0.04$ and the bends $K(\alpha) = \sin^2(\alpha) + 2 \sin^4\left(\frac{\alpha}{2}\right)$. Another K will also be used for the entrance of the injector, which will be specified later on.

For manufacturing costs and simplicity purposes, we choose to only use 45° bends which will result in $K_{bends} = 0.5429$.

With that and the length measurements in mind, we designed the following feeding system layout for which we will then calculate the pressure variations along it :

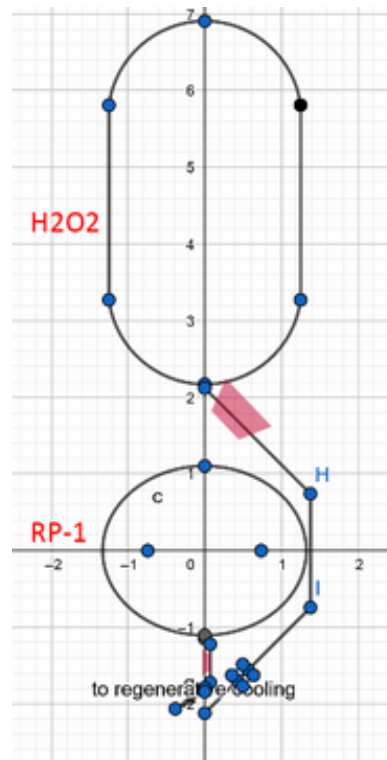


Figure 11.5: Feeding system layout (To scale)

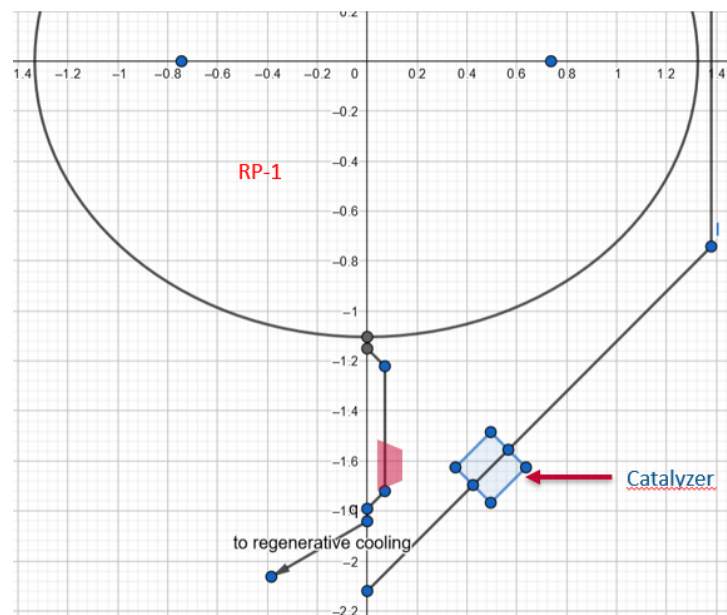


Figure 11.6: Feeding system layout - Zoomed (To scale)

11.6.1 Line diameters

In order to choose our line diameters, we can first use our volume flow and then get the line area from it and then at the end, the line diameter.

Fuel

$$\dot{V}_f = \frac{\dot{m}_f}{\rho_f} = 0.0015298 m^3/s \quad (11.1)$$

$$A_{line_f} = \frac{\dot{V}_f}{w_f} = 5.21 \times 10^{-5} mm^2 \quad (11.2)$$

$$d_{line_f} = 2\sqrt{\frac{A_{line_f}}{\pi}} = 8.1447 mm \quad (11.3)$$

As we are trying to insure a high injection velocity and to insure a certain margin in pressure and velocity, we will choose a line diameter of 7 mm for the fuel feeding system.

Oxidizer

$$\dot{V}_o = \frac{\dot{m}_o}{\rho_o} = 0.006042 m^3/s \quad (11.4)$$

$$A_{line_o} = \frac{\dot{V}_o}{w_o} = 0.000275 mm^2 \quad (11.5)$$

$$d_{line_o} = 2\sqrt{\frac{A_{line_o}}{\pi}} = 18 mm \quad (11.6)$$

In this case, we will choose a line diameter of 15 mm for the oxidizer.

11.6.2 Fuel feeding system

The following items in our fuel feeding system will cause pressure drops :

- Tank exit : $K = 0.04$
- $4 \times 45^\circ$ bends : $K = 0.5429$ for each
- Straight line losses : $\Delta P = \frac{\rho}{2} w^2 f \frac{L}{D}$
- Friction coefficient : $f = 0.02$
- Regenerative cooling : $\Delta P = 0.25$ bar
- Fuel injection : $\Delta P = 9.3843$ bars

With our current layout, we have 5 straight lines which will cause pressure losses on the fuel side. Three of them are before the turbopump which is placed at the end of the

third straight section, right before the third bend. We consider a velocity of 8 m/s before the turbopumps and of $v_{inj} = 29.363$ m/s after. The line loss for each section is given by :

$$\Delta P = \frac{810}{2} w^2 \times 0.02 \times \frac{L_{section}}{0.007}$$

1. First section ($L_{section} = 0.05m$) : $\Delta P = 0.037029$ bar
2. Second section ($L_{section} = 0.1m$) : $\Delta P = 0.074057$ bar
3. Third section ($L_{section} = 0.5m$) : $\Delta P = 0.37029$ bar
4. Fourth section ($L_{section} = 0.1m$) : $\Delta P = 0.997699$ bar
5. Fifth section ($L_{section} = 0.05m$) : $\Delta P = 0.49884$ bar

There are also two different values for the bend losses depending on the position of the bend (before or after the turbopump), we have 2 of each :

- $\Delta P_{before} = 0.14072$ bar
- $\Delta P_{after} = 1.8957$ bar

The tank exit loss is :

$$\Delta P_{exit} = K_{exit} \times \frac{\rho_F}{2} \times 8^2 = 0.010368 \text{ bar}$$

11.6.3 Oxidizer feeding system

The following items in our oxidizer feeding system will cause pressure drops :

- Tank exit : $K = 0.04$
- $4 \times 45^\circ$ bends : $K = 0.5429$ for each
- Straight line losses : $\Delta P = \frac{\rho}{2} w^2 f \frac{L}{D}$
- Friction coefficient : $f = 0.02$
- Catalyzer : $\Delta P = \text{bars}$
- Oxidizer injection : $\Delta P = 4.9599$ bars

On this part of the feeding system, we also have 5 sections and 4 bends of 45° each. We also consider a velocity of 8 m/s before the turbopump and 21.971 m/s after. However, due to the larger distances (due to our tank layout), the turbopump's position in the feeding system is different and is now positioned after the first bend, right at the beginning of

the second straight line. This results in 3 bends being at high velocity and 1 at relatively slower velocity.

Here, each straight line loss section is given by :

$$\Delta P = \frac{1450}{2} w^2 \times 0.02 \times \frac{L_{section}}{0.015}$$

With :

1. First section ($L_{section} = 0.05m$) : $\Delta P = 0.030933$ bar
2. Second section ($L_{section} = 1.95m$) : $\Delta P = 9.0992$ bars
3. Third section ($L_{section} = 1.4836m$) : $\Delta P = 6.9228$ bars
4. Fourth section ($L_{section} = 1.15m$) : $\Delta P = 5.3662$ bars
5. Fifth section ($L_{section} = 0.6m$) : $\Delta P = 2.7997$ bars

For the bends, we have :

- $\Delta P_{before} = 0.2519$ bar (1 of them)
- $\Delta P_{after} = 1.0614$ bar (3 of them)

The tank exit loss is :

$$\Delta P_{exit} = K_{exit} \times \frac{\rho_o}{2} \times 8^2 = 0.01856 \text{ bar}$$

11.7 Turbo pumps

As most of our subsystems have a defined pressure drop due to their specific design, we have made the choice to use this feeding system design with all losses included to then design our turbopumps to have a pressure rise in accordance with our pressure requirements. We chose to go with electrically driven turbo pumps as we have a good amount of electrical power since we use fuel cells in our spacecraft.

Our respective turbopump required created pressures are :

- Fuel side : $\Delta P_{T_f} = P_{Chamber} + \Delta P_{feeding_f} + \Delta P_{inj_f} + \Delta P_{Regenerative \ cooling} - P_{Tank_f}$
- Oxidizer side : $\Delta P_{T_o} = P_{Chamber} + \Delta P_{feeding_o} + \Delta P_{inj_o} + \Delta P_{Catalyzer} - P_{Tank_o}$

Thus,

$$\Delta P_{T_f} = 54.395 \text{ bars} \tag{11.7}$$

$$\Delta P_{T_o} = 102.28 \text{ bars} \tag{11.8}$$

11.8 Pressure evolution summary

11.8.1 Fuel side

Contributor	Pressure Drop (bars)	Pressure at the end of this part (bars)
Tank	NA	1.3
Tank exit	0.010368	1.29
First section	0.037	1.253
First bend	0.14	1.113
Second section	0.074	1.039
Second bend	0.14	0.899
Third section	0.37	0.529
Turbo pump	54.395 (Rise)	54.924
Third bend	1.8957	53.0283
Fourth section	0.997	52.0313
Fourth bend	1.8957	50.1356
Fifth section	0.499	49.6366
Cooling	0.25	49.3866
Injection	9.38	40.0066
Combustion chamber	NA	40.0066

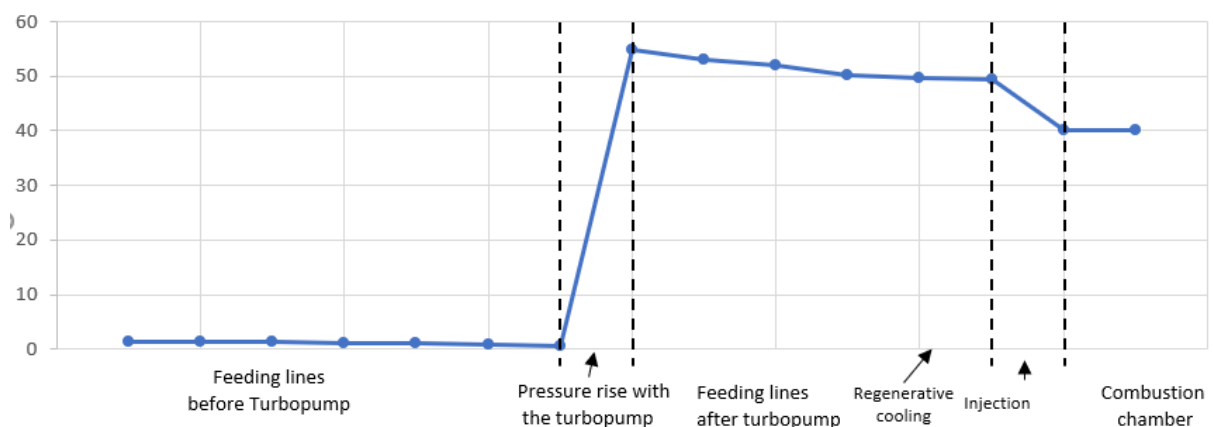


Figure 11.7: Pressure evolution on fuel side (bars)

11.8.2 Oxidizer side

Contributor	Pressure Drop (bars)	Pressure at the end of this part (bars)
Tank	NA	1.3
Tank exit	0.010368	1.29
First section	0.031	1.259
First bend	0.25	1.009
Turbo pump	102.28 (Rise)	103.289
Second section	9.09	94.199
Second bend	1.06	93.139
Third section	6.9228	86.2162
Third bend	1.06	85.1562
Fourth section	5.366	79.7902
Fourth bend	1.06	78.7302
Fifth section	2.7997	75.9305
Catalyzer	30.95	44.9805
Injection	4.96	40.0205
Combustion chamber	NA	40.0205

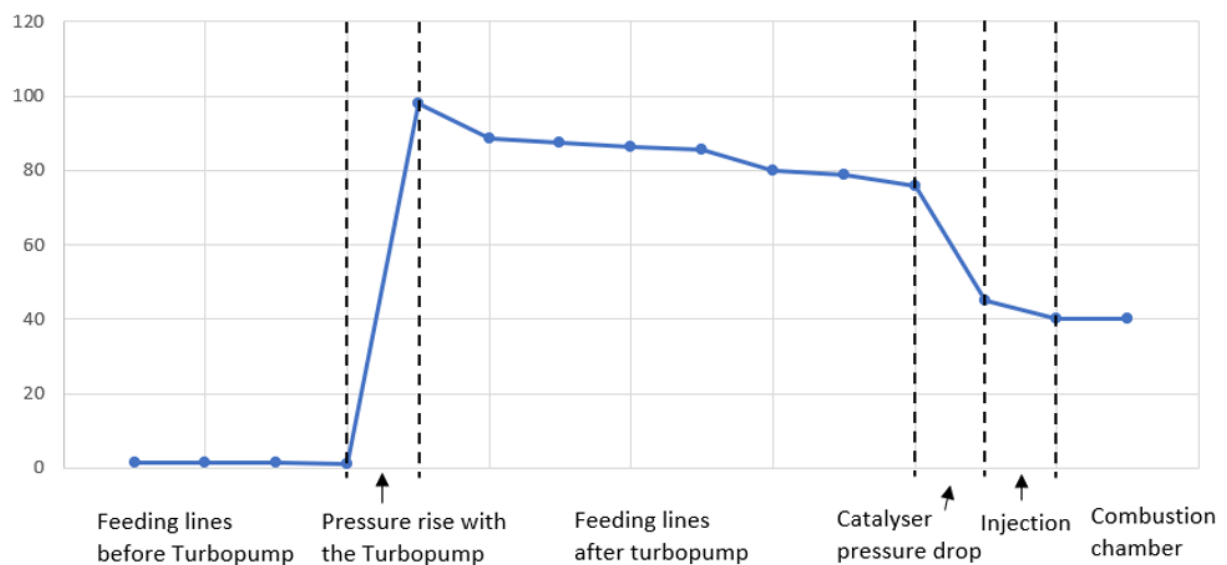


Figure 11.8: Pressure evolution on oxidizer side (bars)

11.9 Engine

11.10 Nozzle

Chapter 12

Simulation

12.1 Subsystem simulation

12.2 System simulation

12.3 Simulation preparation and execution

12.4 Simulation review

Chapter 13

Lessons learnt

Conclusion

List of Figures

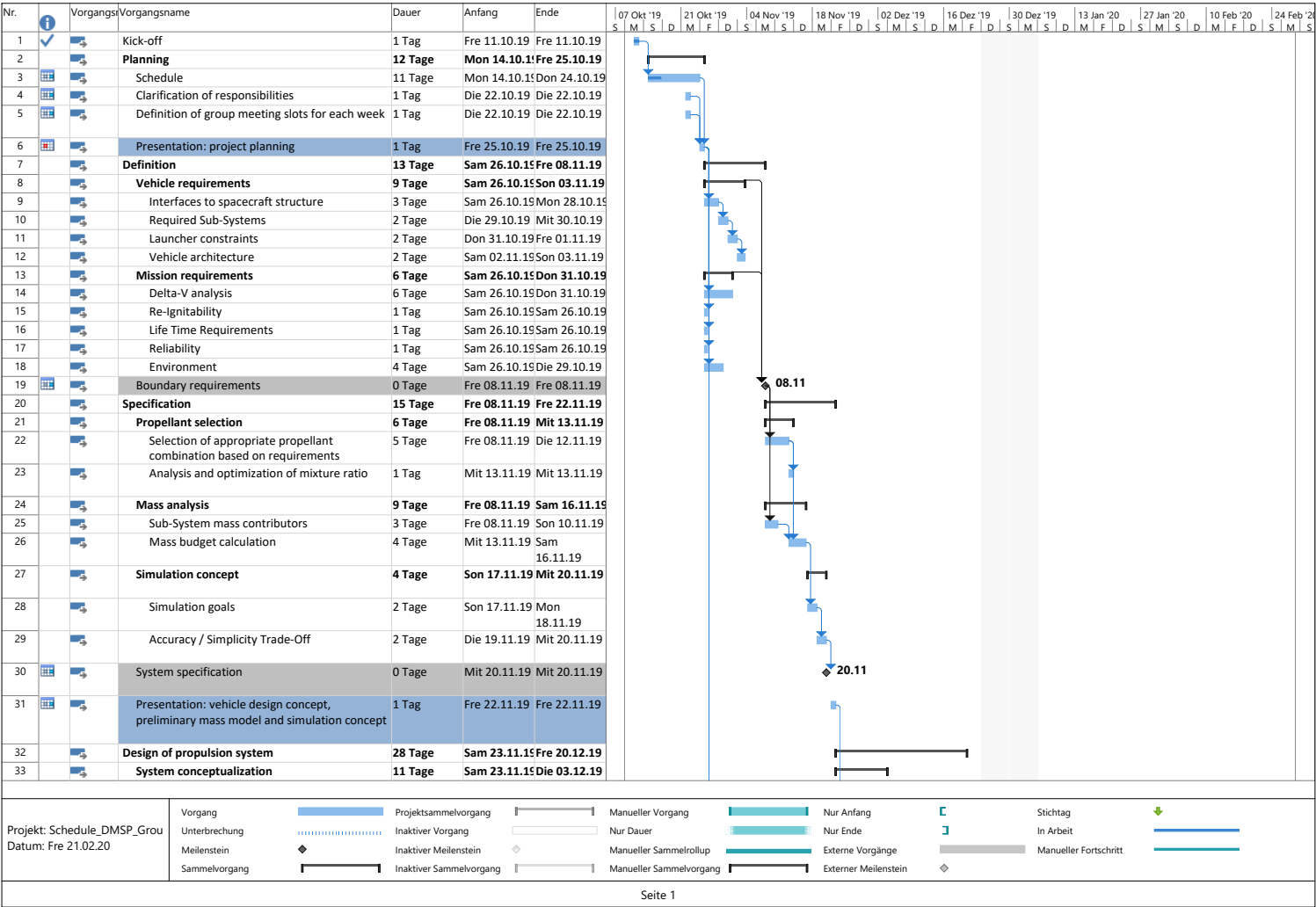
1.1	Initial schedule	3
1.2	Final schedule - comparison as planned and as achieved	4
5.1	CAD of a catching magnet	11
5.2	Catching sequence (not to scale)	12
11.1	H_2O_2 chemical decomposition process	35
11.2	Example of catalyst bed	36
11.3	Pressure drop depending on the size of the catalyst bed	37
11.4	K values for geometry changes	38
11.5	Feeding system layout (To scale)	39
11.6	Feeding system layout - Zoomed (To scale)	39
11.7	Pressure evolution on fuel side (bars)	43
11.8	Pressure evolution on oxidizer side (bars)	44

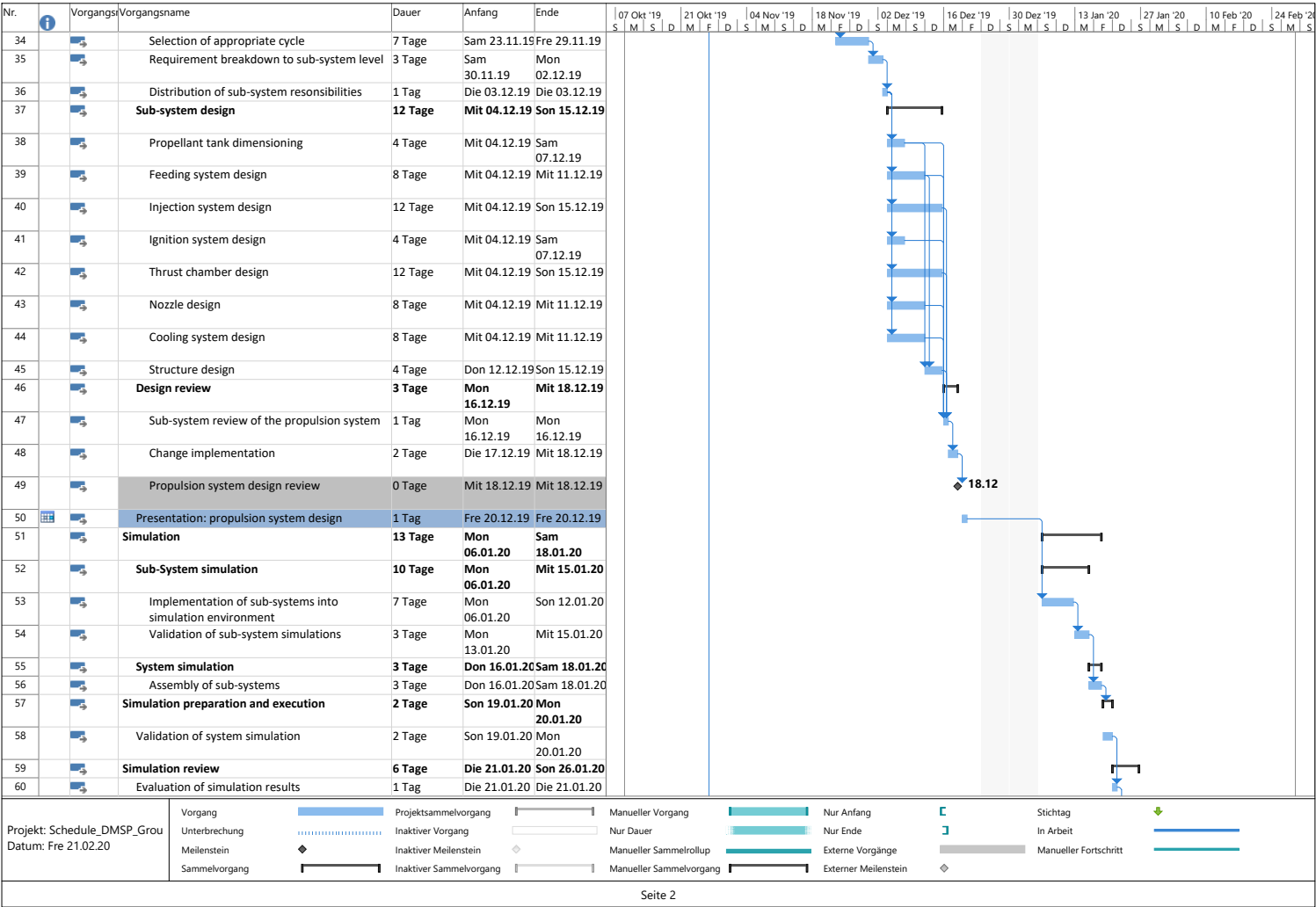
List of Tables

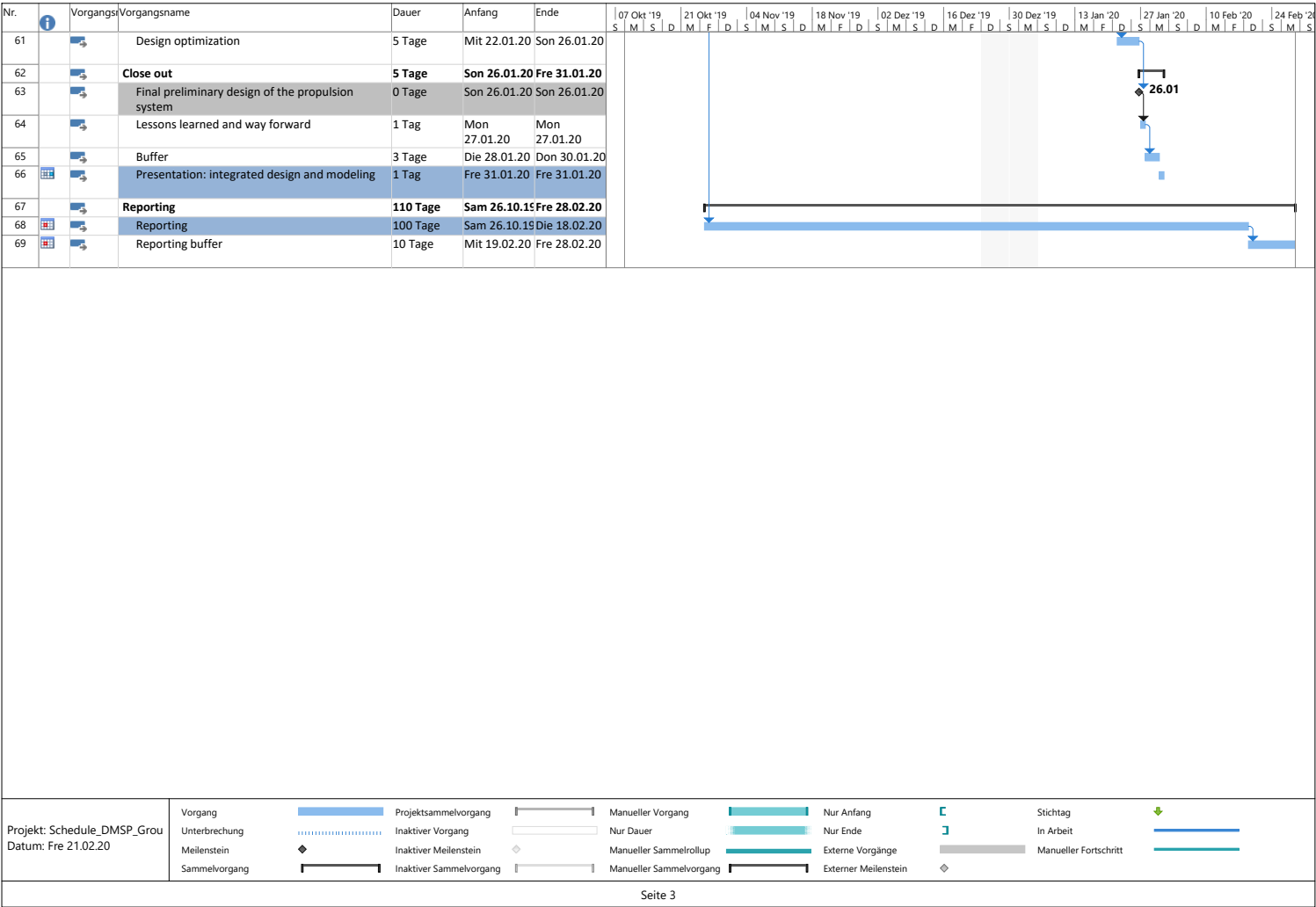
2.1	Requirements for the vehicle	6
7.1	Propellant combinations overview	17
7.2	Detailed propellant comparison MON/MMH and H ₂ O ₂ /RP-1	19
7.3	Historical data of flight H ₂ O ₂ /RP-1 engines	20

Annexes

Annex I - Gantt Diagramm







Sources

1. <http://braeunig.us/space/propel.htm>
2. <http://astronautix.com/l/loxkerosene.html>
3. https://en.wikipedia.org/wiki/Liquid_rocket_propellant#Bipropellants
4. <http://www.astronautix.com/h/h2o2kerosene.html>
5. Hydrogen Peroxide / Kerosene, Liquid-Oxygen / Kerosene, and Liquid-Oxygen / Liquid Methane for Upper Stage Propulsion, Paper, S. Krishnan* Universiti Teknologi Malaysia
6. <https://ntrs.nasa.gov/archive/nasa/casi.ntrs.nasa.gov/19720019028.pdf>
7. https://www.nasa.gov/centers/glenn/technology/fuel_cells.html
8. <https://www.ginerinc.com/regenerative-fuel-cell-systems>
9. <https://ntrs.nasa.gov/archive/nasa/casi.ntrs.nasa.gov/19990063763.pdf>
10. <http://www.esa.int/esapub/bulletin/bullet90/b90dudle.htm>
11. <https://www.sciencedirect.com/science/article/abs/pii/S0360319904003106>
12. <http://citeseerx.ist.psu.edu/viewdoc/download?doi=10.1.1.526.3797&rep=rep1&type=pdf>
13. http://juser.fz-juelich.de/record/135459/files/HP3d_3_Ranjbari.pdf
14. <https://www.sciencedirect.com/topics/chemistry/proton-exchange-membrane-fuel-cells>
15. <http://www.dartmouth.edu/~cushman/courses/engs37/FuelCells.pdf>
16. https://ocw.mit.edu/courses/aeronautics-and-astronautics/16-851-satellite-engineering-fall-2003/lecture-notes/l3_scpowersys_dm_done2.pdf
17. Article : The design and main performance of a hydrogen peroxide/kerosene coaxial-swirl injector in a lab-scale rocket engine
18. Article : Design and Analysis of a Fuel Injector of a Liquid Rocket Engine
19. Article : The spray characteristic of gas-liquid coaxial swirl injector by experiment